applied sciences

MDPI

Article

On the Development of an Intelligent Poly(aniline-co-o-toluidine)/Fe_3O_4/Alkyd Coating for Corrosion Protection in Carbon Steel

Oday I. Mousa [1], Salah S. Al-Luaibi [1], Alaa S. Al-Mubarak [1], Hassane Lgaz [2,*], Belkheir Hammouti [3,4], Abdelkarim Chaouiki [5,*] and Young Gun Ko [5,*]

1 Department of Chemistry, College of Sciences, University of Basrah, Basrah P.O. Box 49, Iraq; oday.mousa@uobasrah.edu.iq (O.I.M.); salahshakir502@gmail.com (S.S.A.-L.); alaa.almubarak@uobasrah.edu.iq (A.S.A.-M.)
2 Innovative Durable Building and Infrastructure Research Center, Center for Creative Convergence Education, Hanyang University ERICA, 55 Hanyangdaehak-ro, Sangrok-gu, Ansan-si 15588, Gyeonggi-do, Republic of Korea
3 Laboratory of Industrial Engineering, Energy and the Environment (LI3E), SUPMTI, Rabat 10000, Morocco; hammoutib@gmail.com
4 Euromed Research Center, Euro-Mediterranean University of Fes, BP 51, Fes 30070, Morocco
5 Materials Electrochemistry Group, School of Materials Science and Engineering, Yeungnam University, Gyeongsan 38541, Gyeongsangbuk-do, Republic of Korea
* Correspondence: hlgaz@hanyang.ac.kr (H.L.); abdelkarim.chaouiki@yu.ac.kr (A.C.); younggun@ynu.ac.kr (Y.G.K.)

Featured Application: Smart corrosion protection systems.

Abstract: The corrosion of metals and alloys presents a significant challenge in many industries, demanding constant maintenance, and thereby increasing costs. In response to this problem, the smart corrosion protection coating has emerged as a promising solution. By enabling the immediate detection of, and response to, environmental changes, such as in the temperature and pH, these smart coatings contribute significantly to extending a material's lifespan, and reducing maintenance expenses. In this study, nanomagnetic [poly(aniline-co-o-toluidine)/Fe_3O_4] systems were prepared and used as a self-healing corrosion inhibitor, mixed with alkyd paint at different weight percentages (5–25%). The composites were used as a coating on carbon steel (C1010), and their corrosion protection performance was tested in 0.1 mol/L HCl, using electrochemical impedance spectroscopy (EIS), scanning electron microscope (SEM), and FTIR analyses. The results showed an adequate corrosion inhibition performance for the developed composites, compared to the alkyd paint alone, reaching an inhibition efficiency of 80% at 20 wt.% of composite. Adding increasing weight percentages of the developed composites to the paints led to a significant increase in the corrosion resistance, accompanied by a remarkable decrease in the double-layer capacitance. Thus, these developed composites show excellent potential as a corrosion protection formulation in paints.

Keywords: corrosion protection; smart coating; alkyd; paint; carbon steel; polyaniline; nanoparticle

Citation: Mousa, O.I.; Al-Luaibi, S.S.; Al-Mubarak, A.S.; Lgaz, H.; Hammouti, B.; Chaouiki, A.; Ko, Y.G. On the Development of an Intelligent Poly(aniline-co-o-toluidine)/Fe_3O_4/Alkyd Coating for Corrosion Protection in Carbon Steel. *Appl. Sci.* **2023**, *13*, 8189. https://doi.org/10.3390/app13148189

Academic Editor: Dimitris Mourtzis

Received: 24 March 2023
Revised: 10 July 2023
Accepted: 10 July 2023
Published: 14 July 2023

1. Introduction

Due to its favorable mechanical and physical properties, low-carbon steel is widely used in a variety of applications. Its excellent weldability and machinability, and relatively low cost, make it a first-choice material in several applications, such as making pipes and structural components in the construction industry; and producing various components, such as beams, frames and supports in the automotive industry [1–3].

Coatings are a widely used corrosion protection method for many metals and alloys [4–7]. Coatings have several advantages and features that make them a better choice

to protect metal from corrosion. Coatings can form a physical barrier that separates the metal from its environment, thus limiting the access to the metal surface of corrosive particles, such as oxygen, chlorides, and other corrosive species [8,9]. Moreover, conversely to other methods, coatings can be applied to a wide range of metallic substrates, such as steels, aluminum, copper, and alloys, and can be customized to meet specific requirements, providing long-term corrosion protection even in highly corrosive environments [8–11]. Furthermore, coatings have the advantage of being cost-effective, particularly when compared to expensive methods, such as material replacement and the repairing of corroded metallic substrates.

Alkyd paints are one of the most used corrosion protection coatings, due to their excellent durability and low-cost. These oil-based paints can be applied to a variety of surfaces using several methods, such as spray, roller, or brush [12]. However, alkyd paint suffers from a low corrosion protection performance, especially when exposed to sunlight and humidity [8,13]. One practical solution to improve the corrosion protection performance of alkyd paints is to incorporate organic or inorganic compounds into the coating formulation [14,15]. Such a practice can significantly improve the barrier properties of the coating, making it more effective in preventing corrosive particles from reaching the metallic substrate. Additives such as nanoparticles can remarkably improve the hardness, adhesion, and durability of the alkyd paint, granting it an excellent resistance to abrasion and scratching, and reduced cracking.

Many researchers have reported smart coatings that show response to a stimulant [16–18]. Smart paint can include different responses, such as self-healing, self-cleaning, corrosion-sensing, and anti-fouling, among others [19]. Among smart-coating technologies, the concept of self-healing coating was introduced as a new approach to achieving corrosion protection function. The automatic corrosion response can be designed according to various factors, such as abrasions, pH change, surface tension, and temperature. Self-repairing organic and inorganic coatings can increase the functional life of the resulting coating structure. The self-healing function can be transported, due to the presence of nano/microcontainers of polymers and inorganic particles in paint structures [20].

Magnetic nanoparticles are of great importance to researchers because of their wide range of applications, which cover many research fields, including catalysts, biotechnology, biomedicine, and data storage [14,21,22]. They possess excellent characteristics, such as a small size, high surface area-to volume ratio, and biocompatibility, making them the best option for many applications. The successful application of these particles depends on the stability of molecules under different conditions. For instance, the performance of magnetic nanoparticles is better when the particle size is less than the critical value.

Because of the significant losses that result from the high corrosion rate of metals and alloys in corrosive acidic environments, the mechanism of corrosion protection in alloys and metals has gained a high importance, due to its durability in these environments [23]. Consequently, the protection of metals and alloys using organic coatings is of great importance to reducing corrosion [24–27]. Microsize commercial pigments are used in the coating systems, and have an essential effect on the organic coating properties. However, these coatings are not guaranteed to be free of defects and problems [28]; for example, ineffective adhesion problems, reduced coating elasticity, shock resistance loss, lower wear resistance, and low resistance to corrosion. Therefore, to overcome these defects and improve the coating's performance, nanopolymers can be involved in the coating; this is considered to be a modern method. These materials show a tremendous improvement in properties compared to traditional coatings, because of the small size of their particles. Moreover, the nanomaterials utilized in the coatings and the production of the coatings provide multiple functions [29].

Riaz et al. have reported the development of nanostructured polyaniline (PANI) and poly(1-naphthylamine) (PNA) incorporated into soya oil alkyd, and their corrosion protection performance [30]. Authors have monitored the anti-corrosion properties of developed composites using weight loss, electrochemical tests, and scanning electron microscopy. Elec-

trochemical tests showed that the developed PNA/Alkyd composite exhibited the highest corrosion protection performance. Jadhav et al. have studied the synthesis of nanopolyaniline (PANI) and poly-o-anisidine (POA), using the emulsion polymerization method in a micellar solution of SDS, and then their impregnation into alkyd paint, to improve its corrosion protection ability [31]. The anti-corrosion studies using the weight loss method showed that the nano PANI/Alkyd composite demonstrated excellent corrosion protection compared to POA/Alkyd coatings. The authors also reported a significant improvement in the scratch hardness of both coatings, compared with the pristine alkyd coating. On the other hand, Jeyasubramanian et al. [15] studied the preparation and characterization of nano-iron oxide, and its impregnation into alkyd coatings for corrosion protection improvement. The authors reported excellent anti-corrosion properties in the developed coating formulation for steel in a 3.5% NaCl solution. Other successful applications of metallic nanoparticles incorporated into alkyd coatings have been reported in a recent publication by Ifijen et al. [14].

In this research, an acrylic polyurethane (APU) coating, which consists of two components, an isocyanate in combination with nanomagnetite particles, was used. Magnetite, which has a high magnetic susceptibility, is highly adherent to the metal surface [32]. Magnetite is a magnetic oxide that can be prepared in various ways, including the co-precipitation method. It can also be produced from the interaction of iron and trioxide, as shown in the following equation:

$$\underset{\text{Ferrous Oxide}}{FeO} + \underset{\text{Ferric Oxide}}{Fe_2O_3} \rightarrow \underset{\text{Magnetite}}{Fe_2O_4}$$

Drawing inspiration from similar studies on nanocomposites, the mechanical characteristics of these developed composites could potentially include an enhanced fracture toughness, superior strength-to-weight ratio, high tensile properties, increased fatigue resistance, and improved corrosion resistance to severe environments [33–35]. Additionally, based on analogous studies, as the weight percentage of nanomagnetic systems increases, there could be a significant enhancement in the material's mechanical behavior, similar to the linearly increasing Young's modulus and flexural modulus observed in certain studies when filler materials were added [36–39].

The combination of the APU coating with nanomagnetic poly(aniline-co-o-toluidine) can be performed via copolymer, which is considered as a novel morphology, with better thermal stability and higher solubility compared to its homopolymers [40]. Juliet et al. reported the characterization of copolymerization for aniline-co-o-toluidine and V_2O_5 nanocomposites [41]. Its unique properties have been reported, such as an easy preparation method at a low cost [42], and its high resistance to corrosion. The prepared composites were characterized using scanning electron microscopy (SEM) and FTIR analyses. Furthermore, electrochemical impedance spectroscopy (EIS) was used to evaluate the effects of adding copolymer poly(aniline-co-o-toluidine)/iron oxide magnetic nanoparticle composites to the alkyd paint on the corrosion protection of carbon steel, in an acidic medium. The prepared composites were added in different weight percentages, ranging from 5 to 25 wt.%.

2. Materials and Methods

2.1. Raw Materials

Several chemicals from various companies were used in this study, such as aniline, Ferric chloride hexahydrate and ferrous sulfate heptahydrate, ortho toluidine, hydrochloric acid, and sodium persulfate. The alkyd paint and carbon steel alloy (Grade C1010) were supplied by the local market. The physical properties of the alkyd paint and carbon steel composition are shown in Tables 1 and 2, respectively. Aniline and o-toluidine monomers were distilled before use, under reduced pressure. No further treatments were carried out for the other used reagents. All chemicals were supplied by BDH chemicals (Poole, UK),

except for $FeCl_3 \cdot 6H_2O$ and $FeSO_4 \cdot 7H_2O$, which were sourced from Merck Co. (Darmstadt, Germany). The aniline and O-Toluidine were freshly distilled before polymerization.

Table 1. The physical properties of the alkyd paint used in the present work.

Shade No./Color	Finish	Solids Volume, %	Theoretical Spreading Rate	Flashpoint
Grey 12170	Matt Surface dry 4 h (10 °C)	Grey 12170: 48% Through-dry 12 h (10 °C)	10.8 m^2/L - 0.035 mm Volatile organic compounds content 405 g/L	>35 °C Specific gravity 1.26 kg/L

Table 2. The chemical composition of the carbon steel used (in wt.%).

C%	S%	Mn%	P%	Si%	Cr%	Ni%	Cu%	As%	Fe%
0.083	0.002	0.50	0.003	0.011	0.019	0.0111	0.0183	0.097	99.1

2.2. Synthesis of Copolymer Poly(aniline-co-o-toluidine)

Firstly, 0.27 mol of aniline monomer was dissolved in 27 mL of 1 mol/L HCl, and 0.27 mol of o-toluidine monomer was dissolved in 27 mL of the same acid. Then, the monomers were placed in a 250 mL round-bottom flask. Next, 32 mL of sodium persulfate (SPS) solution was added dropwise to the monomer mixture. The reaction mixture was continuously stirred for two hours. The reaction mixture temperature was set between 0 °C and −5 °C. The copolymer obtained from the previous test was washed by distilled water and filtered. A dark green precipitate was acquired and then dried at 60 °C in a vacuum [43].

2.3. Synthesis of Magnetite Nanoparticles (Fe_3O_4)

Iron oxide nanoparticles were prepared based on the co-precipitation of Fe^{3+} and Fe^{2+}, with a molar ratio of 2:1, respectively [44], and 2.7 g of $FeCl_3 \cdot 6H_2O$ and 1.2 g of $FeSO_4 \cdot 7H_2O$, were dissolved in 100 mL of deionized water under nitrogen. The mixture was vigorous stirred, using a magnetic stirrer, at 80 °C for one hour. Then, 15 mL of 32% ammonium hydroxide was added to the mixture gradually, dropwise, with the reaction mixture constantly stirred. After the ammonium hydroxide was added, a precipitate was produced instantly [45]. The dark precipitate was washed six times, with the distilled water to remove excess ammonium ions. Finally, the humid suspension was evaporated, and dried for 24 h.

2.4. Synthesis of Copolymer Poly(aniline-co-o-toluidine)/Iron Oxide Magnetic Nanoparticle Composites

Poly(aniline-co-o-toluidine)/Fe_3O_4 magnetic nanoparticles composites were prepared [46] by adding 1 mol/L of pre-prepared co-polymer poly (aniline-co-o-toluidine) to the reaction mixture containing 2 mol/L of aqueous ferric chloride, 1 mol/L of aqueous ferrous sulfate, and 100 mL of distilled water. The mixture was placed in a three-necked round-bottom flask, equipped with a mechanical stirrer. The reaction was carried out at a temperature of 80 °C, for one hour, in an inert atmosphere. Then, the mixture was cooled, and 15 mL ammonium hydroxide solution at 32% concentration was added to the mixture as drops, gradually, and the nanomagnetic particles were precipitated. In order to remove excess ammonium ions, the precipitate was washed several times in distilled water. The humid suspension eventually evaporated, and dried for 24 h. After the drying process, copolymer/Fe_3O_4 nanocrystals were ground. In the same way, the copolymer poly(aniline-co-o-toluidine)/Fe_3O_4 magnetic nanoparticles were prepared. This method is called co-precipitation and, through it, the magnetic nanoparticles of the copolymer were obtained.

2.5. Preparation of the Carbon Steel

In this study, the carbon steel alloy C1010 was used; its components are shown in Table 2. It was washed with distilled water several times, then washed with ethanol and acetone to remove traces of water. Next, the alloys were polished using very fine silicon carbide sheets (600–3000) and, in the presence of alumina (Al_2O_3), a smooth and shiny surface was obtained for the alloy. Then, the ingot was cleaned using a cloth, and washed with distilled water and ethanol once again. It was immersed in acetone for a short time, then raised and left to dry in the air, and then kept in a glass dryer.

2.6. Coating of the Carbon Steel

The alloy was first coated with alkyd paint alone; a weight of 0.3 g of paint was taken, then distributed homogeneously over a 1 cm^2 area of the alloy's surface. A small area of the alloy was left without coating, for electrical contact with the working electrode. Then, the second model was coated with Fe_3O_4, taking a weight of 5%w/w, which corresponds to a weight of 0.015 g of Fe_3O_4, and 0.285 g of the alkyd paint, mixed homogeneously, and this was repeated with the rest of the percentages (10, 15, 20, and 25%w/w) of the coating mixture. Then, with the same percentages as above, the alkyd paint was mixed with the prepared copolymer [poly(aniline-co-o-toluidine)/Fe_3O_4] MNPs, while being mixed at (25%w/w) with the copolymer poly (aniline-co-o-toluidine). The coating thickness of the samples was maintained, at an average of 40 μm, with a tolerance of ±5 μm. To ensure uniformity across all samples, the same amount of coating material was applied to each. Furthermore, the samples were dried under identical conditions, and they were placed on a level surface, to maintain consistency during the drying process.

2.7. Electrochemical Impedance Spectroscopy

Electrochemical impedance spectroscopy (EIS) is a non-destructive technique used to study the electrical properties of materials in electrochemical systems. It involves applying a small AC voltage to the system, and measuring the resulting current response, over a range of frequencies. By analyzing the impedance data, EIS can provide information on parameters such as the resistance, capacitance, and charge transfer processes in the system, making it a powerful tool for studying corrosion and other electrochemical processes. To perform electrochemical measurements, a classical setup, consisting of a single-compartment glass cell and a three-electrodes system, was used. The system was composed of a reference electrode (saturated calomel (SCE)), a counter electrode made from a platinum grid with a large surface area, and a working electrode made from carbon steel, employing the Corrtest potentiostat/galvanostat model CS350, controlled by CS Studio5software. The electrochemical impedance spectroscopy (EIS) tests for the carbon steel immersed in 0.1 mol/L HCl, both with and without the formulations, were carried out, applying an alternating current within the frequency range of (0.01–105) Hz, and using an AC signal of 10 mV. Prior to the EIS tests, the open circuit potential (OCP) was monitored, until a stable potential was achieved, ensuring that the system had reached a steady state, and thereby providing a more accurate reflection of the corrosion behavior under equilibrium conditions.

2.8. Characterization Techniques

Fourier-transform infrared spectroscopy analysis was performed using a Perkin Elmer Spectrum 100 FT-IR Spectrometer (PerkinElmer, Waltham, MA, USA). In this technique, infrared radiation was passed through a sample, and the absorbance was measured at various wavelengths, to yield an infrared spectrum. The spectra were recorded in the wavenumber range of 4000–400 cm^{-1}, at a resolution of 4 cm^{-1}. Scanning electron microscopy was used to examine the morphological structure and topography of the coatings. The analyses were conducted using a Zeiss EVO MA10 (Carl Zeiss AG, Oberkochen, Germany) scanning electron microscope.

3. Results and Discussion

3.1. FT-IR Analysis

The FT-IR spectra of Fe_3O_4 MNP_S and [Poly(aniline-co-o-toluidine)/Fe_3O_4] MNP_S are shown in Figure 1a,b, respectively. It can be seen from Figure 1a that the characteristic absorption of the Fe-O bond is at 570 cm^{-1}, whereas in the copolymer, it appears at 582 cm^{-1}. As shown in Figure 1b, the characteristic peak at 3321 cm^{-1} is related to the N-H stretching of the primary amine, and proves the amino group copolymer [43]. The peak at 2920 cm^{-1} is attributed to the C-H stretching vibration of the methyl group of the copolymer. The absorption peak at 1589.40 cm^{-1} is assigned to the quinoid ring stretching for Poly(aniline-co-o-toluidine) MNPs. The peak observed at 1496 cm^{-1} corresponds to the presence of the C=C stretching vibration in the benzenoid ring in the copolymer. The sharp peaks at 1149.61 cm^{-1} and 813.99 cm^{-1} correspond to the C-H bending in-plane and out-plane, respectively, in the copolymer. The peak at 1300 cm^{-1} corresponds to the C-N stretching vibrations of the primary aromatic amine in the Poly(aniline-co-o-toluidine) MNP_s. The peak at 1242 cm^{-1} is attributed to the C-N stretch of the benzenoid ring C-N-C.

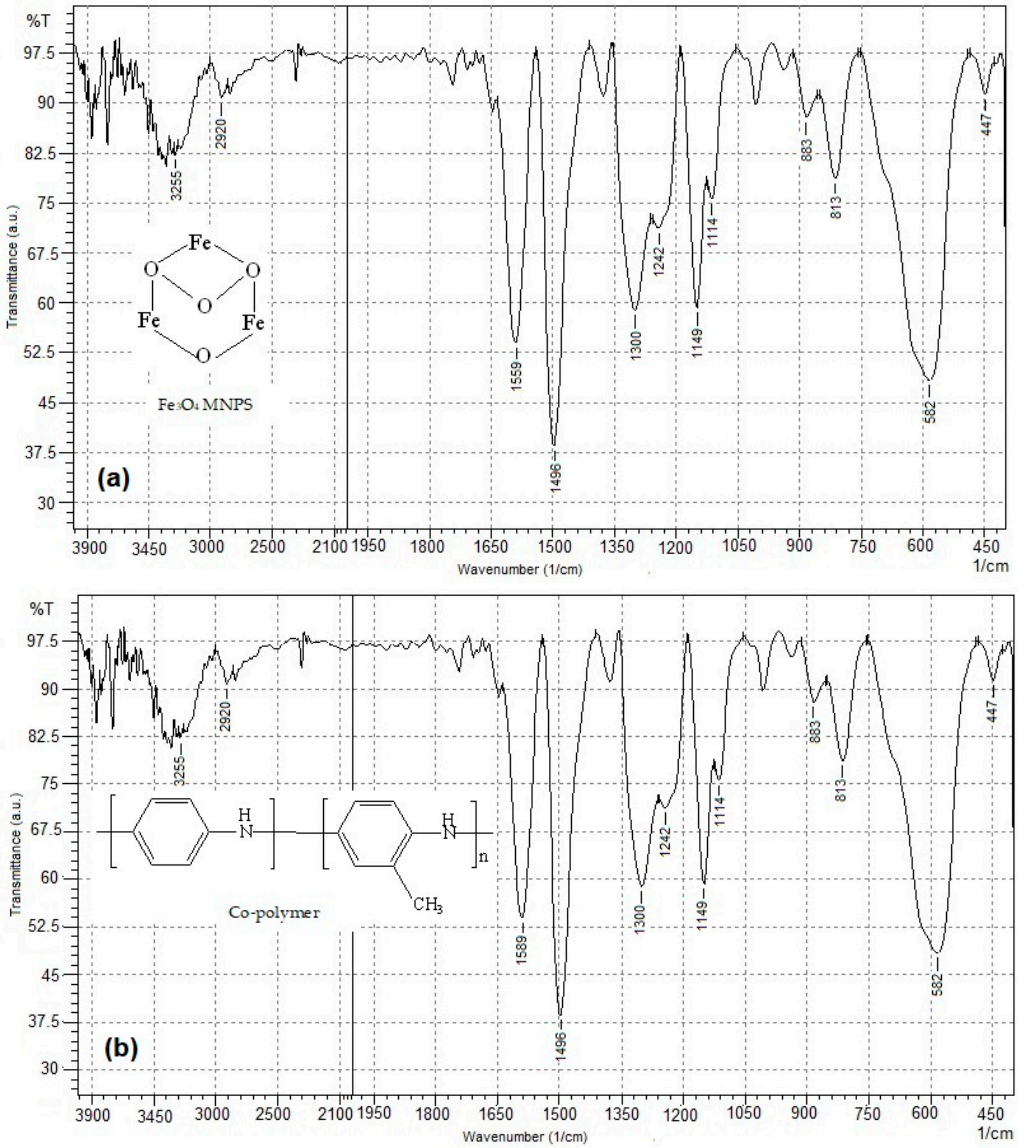

Figure 1. The FTIR spectrum of (**a**) as-prepared (Fe_3O_4) MNPs, and (**b**) as-prepared [Poly(aniline-co-o-toluidine)/Fe_3O_4] MNPs.

3.2. SEM Analysis

Figure 2a,b present the SEM images of Fe_3O_4 MNPs and [Poly(aniline-co-o-toluidine)/Fe_3O_4] MNPs, respectively. Upon analysis, the nanoparticle sizes appear to fall within the range of 29.95 nm to 49.60 nm. Significantly, the size distribution is narrow, pointing toward a controlled synthesis and a uniformity in the particle size. Furthermore, a close examination of the particle morphology shows a consistent and well-defined shape throughout the samples. This uniform morphology could potentially contribute to enhanced physical and chemical properties in the resulting composite materials, making them suitable for corrosion protection. The detailed features highlighted in the SEM images underline the material's potential for use as an effective corrosion protection material.

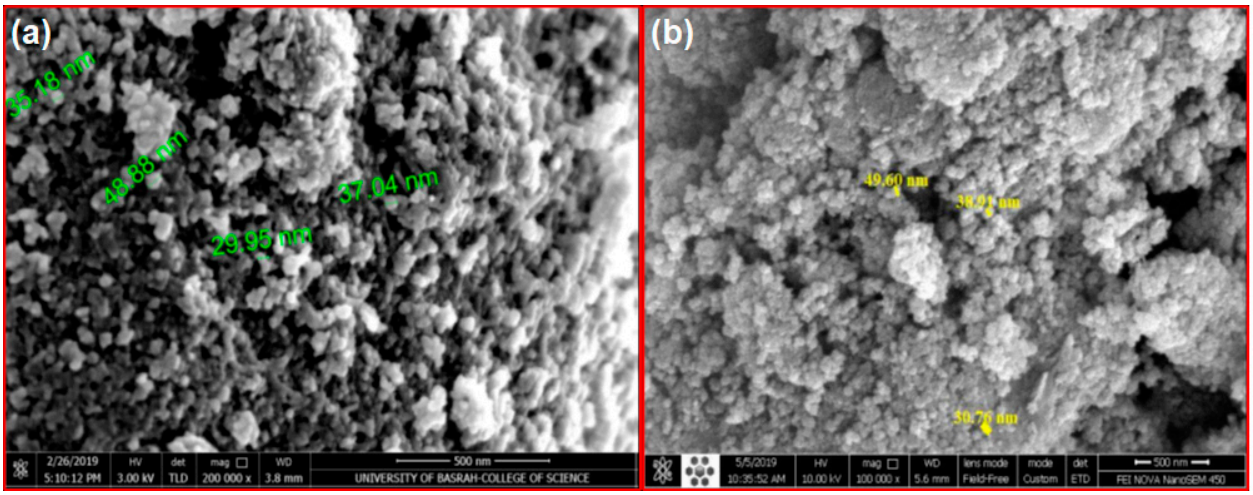

Figure 2. SEM images of (**a**) Fe_3O_4 MNPs, and (**b**) [Poly(aniline-co-o- toluidine)/Fe_3O_4]MNPs.

3.3. Corrosion Resistance Performance

The corrosion protection capabilities of the materials prepared can be effectively evaluated using electrochemical impedance spectroscopy (EIS) tests. The EIS data is graphically represented via Nyquist and Bode plots, as depicted in Figure 3 and the Supplementary Materials. To further scrutinize the electrochemical impedance characteristics, the collected data were processed utilizing CS Studio, specifically employing the Z-view function to extract additional pertinent information. This technique yields two types of visual outputs: Nyquist and Bode plots. These plots depict the behavior of the carbon steel alloy coated with specific weight ratio mixtures of Fe_3O_4 MNPs and [Poly(aniline-co-o-toluidine)/Fe_3O_4] MNPs, combined with alkyd resin, in a 0.1 mol/L HCl solution.

The analysis of the experimental EIS results involves multiple variables, all of which are included in Table 3. These variables include the solution resistance (R_s), the polarization resistance of the metal surface (R_p), which signifies protective properties, and the constant phase element (CPE) [47]. The phase shift (n) serves as a measure of the metal surface roughness. The double-layer capacitance (C_{dl}) forms a layer due to the coating on the solution's surface, and as calculated using Equation (1) [48–51]:

$$C_{dl} = 1/(2\pi R_p f_{max}) \quad (1)$$

The efficacy of the prepared coatings can be evaluated from the corrosion protection efficiency (η%), calculated using Equation (2):

$$\eta(\%) = \left(\frac{Rp_{inh} - R_p}{Rp_{inh}}\right) \times 100 \quad (2)$$

where R_{pinh} and R_p represent the polarization resistance with and without the presence of particles, respectively. The relaxation time (τ) values can be computed using Equation (3) [52]:

$$\tau = C_{dl}R_P \quad (3)$$

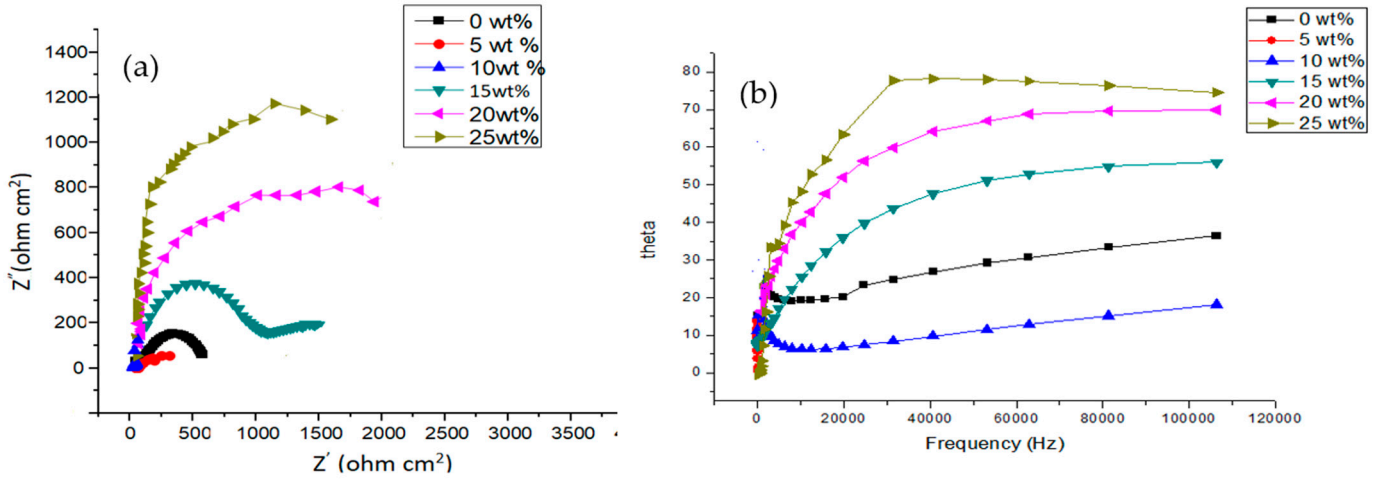

Figure 3. (**a**) Nyquist plot, and (**b**) Bode plot of [Poly(aniline-co-o-toluidine)/Fe_3O_4] MNPs with alkyd paint for carbon steel, in 0.1 mol/L HCl at 298 K.

Table 3. The EIS parameters for the coated alloy in the presence of [poly(aniline-co-o-toluidine)/Fe_3O_4] MNPs and magnetite with alkyd paint in 0.1 mol/L HCl at 298 K.

Formulation	Wt.% of Inhibitor	R_p (Ω cm^2)	n	$Y_\circ \times 10^{-5}$ (Ω^{-1} S^n cm^{-2})	$C_{dl} \times 10^{-7}$ (μF cm^{-2})	τ (s)	f_{max} (Hz)	% IE
Alkyd	-	577.2	0.5707	7.598	1.04×10^3	0.67	236.69	-
Fe_3O_4 MNPs	5	986.1	0.4287	10.437	5.23	0.12	1263.7	41
	10	1073	0.5286	0.024	2.79×10^{-3}	0.02	5441.2	46
	15	1143	0.7363	0.022	7.94	0.18	856.72	50
	20	1235	1.201	0.001	1.76×10^3	0.21	734.38	53
	25	1304.7	1.079	0.004	1.06×10^3	0.10	1508	56
[Poly(aniline-co-o-toluidine)/Fe_3O_4]	5	1167	1.294	0.026	6.98×10^4	0.61	258.61	50
	10	1195	0.1138	5.117	1.64×10^{-28}	7.96	20.934	52
	15	2651	0.2900	1.158	3.58×10^{-8}	3.90	40.792	78
	20	2810	0.6795	0.039	1.31	2.77	23.365	80
MNPs	25	2749	0.8284	0.040	68.7	0.39	404.57	79

The EIS data depicted in Figure 3a, Figures S1a and S2a (Supplementary Material) show that the Nyquist plots' semicircles of the copolymer[poly(aniline-co-o-toluidine)/Fe_3O_4] MNPs combined with alkyd paint at different weight proportions (5–25% *w*/*w*) are significant, compared to the plots of magnetite (Fe_3O_4) and non-magnetized poly(aniline-co-o-toluidine) when mixed with alkyd paint. This signifies an enhanced corrosion protection efficiency for [poly(aniline-co-o-toluidine)/Fe_3O_4] MNPs. An increase in polarization resistance implies an increased corrosion protection efficiency. Nyquist plots display only a single capacitive semicircle in the entire frequency range, indicating a singular time constant associated with the charge transfer process [53–56]. Corresponding Bode plots confirm this one-time constant behavior. The application of the coating on the carbon steel yields an increased value of phase angle, suggesting an excellent anti-corrosion efficiency [57].

The addition of magnetite and [Poly(aniline-co-o-toluidine)/Fe_3O_4] MNPs to the alkyd coating at various weight percentages does not alter the corrosion mechanism. Instead, it amplifies the surface coverage, and enhances the coating's efficiency and corrosion protection ability. This improves the coating's barrier properties, and boosts the adhesive force of the coating on the metal surface, hence physically isolating the metal alloy from the corrosive medium [58,59]. The physical separation signifies the coating's efficiency when

combined with magnetic nanoparticles, effectively impeding the penetration of corrosive particles, such as water molecules, oxygen, and other ions [60]. A higher percentage of corrosion inhibitor improves the inhibitory efficiency. The values of R_p also rise with an increased percentage of Fe_3O_4 MNPs and [Poly(aniline-co-o-toluidine)/Fe_3O_4] MNPs, as indicated in Table 3. This elevation in R_p values results in a corrosion reduction and efficiency augmentation [61]. However, a decreased inhibitory efficiency may be noticed at certain inhibitor weight percentages, due to the potential deterioration of the coating layer caused by surface roughness, heterogeneity, and possible structural deformation [62]. The adsorption of the Fe_3O_4 inhibitor and the copolymer [Poly(aniline-co-o-toluidine)/Fe_3O_4] MNPs on the corroded alloy surface impedes charge transport, and obstructs corrosion-prone active sites, leading to an R_p increase from 577.2 kΩ cm^2 (with the alkyd alone) to 1304.7 and 2749 kΩ cm^2 (with 25 wt.% of Fe_3O_4 and the copolymer [Poly(aniline-co-o-toluidine)/Fe_3O_4] MNPs, respectively). This significant effect contributes to a substantial corrosion rate reduction, thus providing effective protection for the steel surface.

The data displayed in Table 3 exhibit a substantial reduction in C_{dl} (double layer capacitance) values upon application of the treated coatings, compared to using alkyd resin alone. This indicates that the incorporated inhibitors, both magnetite and [copolymer/Fe_3O_4] MNPs, are effective in hindering the corrosion rate of alloys by implementing an adsorption mechanism, and thereby mitigating the extent of metal dissolution. The decreased C_{dl} values associated with the highest percentages of both magnetite and [copolymer/Fe_3O_4] MNPs can be attributed to a lower dielectric constant, and an increase in the double layer thickness, due to the adsorption of these particles on the carbon steel surface. The value of C_{dl} correlates with the thickness of the protective layer, as expressed using the following equation:

$$C_{dl} = \frac{\varepsilon\ \varepsilon_{\circ} A}{d} \quad (4)$$

where (ε) represents the local dielectric constant of a solution, ($\varepsilon_{\circ}$) is the permittivity of free space, (d) is the protective layer thickness, and (A) is the electrode surface area [63].

Furthermore, the variable n, representing phase displacement, provides information regarding the surface characteristics of the coating; a lower n value implies a rougher surface, while a higher value indicates a smoother, more uniform surface [64,65]. As evidenced in Table 3, the highest n value was found at a 25% concentration for the copolymer compound, whereas the maximum n value for the magnetite compound was observed at a 20% concentration. These atypical or irregular n values could be due to variations in the coating properties at different concentrations. Changes in thickness, uniformity, and porosity can cause deviations from the expected linear trends. The higher n values imply a denser adsorption of inhibitor particles on the alloy surface, subsequently slowing down the alloy's corrosion process, and enhancing the inhibition efficiency, with an increase in the inhibitor weight percentage. It is important to note, however, that such irregularities in n and Q values emphasize the complexity of the system, and could also hint at variations in the coatings' physical properties. These unexpected trends underscore the necessity for further microlevel investigations of coatings, to better understand and optimize their performance.

4. Conclusions

This research has demonstrated the effective application of magnetic [poly(aniline-co-o-toluidine)/Fe_3O_4] nanoparticles and magnetite (Fe_3O_4), in combination with alkyd paint, as a novel coating for corrosion protection in carbon steel in acidic environments. The magnetic nanoparticles and magnetite were blended with alkyd resin in varying percentages (5–25%). The electrochemical impedance spectroscopy (EIS) results revealed that this innovative coating offered superior protection against corrosion, compared to alkyd paint alone.

Furthermore, the coatings incorporating the copolymer [poly(aniline-co-o-toluidine)/Fe_3O_4] nanoparticles displayed a higher inhibition efficiency than those mixed solely

with magnetite. This improved performance was attributed to an increased polarization resistance (R_p), which was particularly noticeable at the maximum inhibitor percentage. As the inhibitor percentage increased, the coating's wear resistance was enhanced, forming a more robust protective layer on the carbon steel surface.

The novel coating also demonstrated the capacity to reduce electrical capacitance, indicating its potential for displacing adsorbed water molecules or ions on the metal surface. The adhesive force of the coating on the metal alloy surface was notably improved when using the alkyd with [poly(aniline-co-o-toluidine)/Fe_3O_4] nanoparticles, creating a physical barrier between the alloy and the corrosive medium, and inhibiting electrolyte solution penetration.

The findings from this research open promising avenues for the development of smart corrosion protection strategies for carbon steel.

Supplementary Materials: The following supporting information can be downloaded at: https://www.mdpi.com/article/10.3390/app13148189/s1, Figure S1: (a) Nyquist plot, (b) Bode plot of poly (aniline-co-o-toluidine) with Alkyd paint for carbon steel in 0.1 M HCl at 298K; Figure S2: (a) Nyquist plot; (b) Bode plot of Fe3O4 MNPS with Alkyd paint for carbon steel in 0.1 M HCl at 298K.

Author Contributions: Conceptualization, methodology, software, validation, formal analysis, writing—original draft preparation, O.I.M., S.S.A.-L., A.S.A.-M. and H.L.; investigation, resources, data curation, writing—review and editing, A.C. and H.L.; visualization, supervision, project administration, funding acquisition, B.H. and Y.G.K. All authors have read and agreed to the published version of the manuscript.

Funding: This research received no external funding.

Institutional Review Board Statement: Not applicable.

Informed Consent Statement: Not applicable.

Data Availability Statement: The data cannot be shared at this time as the data also forms part of an ongoing study.

Conflicts of Interest: The authors declare no conflict of interest.

References

1. Deyab, M.A.; Zaky, M.T.; Nessim, M.I. Inhibition of Acid Corrosion of Carbon Steel Using Four Imidazolium Tetrafluoroborates Ionic Liquids. *J. Mol. Liq.* **2017**, *229*, 396–404. [CrossRef]
2. Swetha, G.A.; Sachin, H.P.; Guruprasad, A.M.; Prasanna, B.M.; Sudheer, K. Use of Seroquel as an Effective Corrosion Inhibitor for Low Carbon Steel in 1 M HCl. *J. Bio-Tribo-Corros.* **2018**, *4*, 57. [CrossRef]
3. Lgaz, H.; Salghi, R.; Ali, I.H. Corrosion Inhibition Behavior of 9-Hydroxyrisperidone as a Green Corrosion Inhibitor for Mild Steel in Hydrochloric Acid: Electrochemical, DFT and MD Simulations Studies. *Int. J. Electrochem. Sci.* **2018**, *13*, 250–264. [CrossRef]
4. Shi, H.W.; Liu, F.C.; Han, E.H.; Wei, Y.H. Effects of Nano Pigments on the Corrosion Resistance of Alkyd Coating. *J. Mater. Sci. Technol.* **2007**, *23*, 551–558.
5. Li, J.; Ecco, L.; Fedel, M.; Ermini, V.; Delmas, G.; Pan, J. In-Situ AFM and EIS Study of a Solventborne Alkyd Coating with Nanoclay for Corrosion Protection of Carbon Steel. *Prog. Org. Coat.* **2015**, *87*, 179–188. [CrossRef]
6. Ecco, L.G.; Fedel, M.; Ahniyaz, A.; Deflorian, F. Influence of Polyaniline and Cerium Oxide Nanoparticles on the Corrosion Protection Properties of Alkyd Coating. *Prog. Org. Coat.* **2014**, *77*, 2031–2038. [CrossRef]
7. Deyab, M.A.; Keera, S.T. Effect of Nano-TiO_2 Particles Size on the Corrosion Resistance of Alkyd Coating. *Mater. Chem. Phys.* **2014**, *146*, 406–411. [CrossRef]
8. Wang, H.; Hu, G.; Liu, X.; Guo, L.; Li, X.; Guo, R.; Li, Y. Concurrent Alkylation and Crosslinking of Polyaniline for Enhanced Anticorrosive Performance of Waterborne Alkyd Coating. *Prog. Org. Coat.* **2022**, *168*, 106865. [CrossRef]
9. Piao, J.; Wang, W.; Cao, L.; Qin, X.; Wang, T.; Chen, S. Self-Healing Performance and Long-Term Corrosive Resistance of Polyvinylidene Fluoride Nanofiber Alkyd Coating. *Compos. Commun.* **2022**, *36*, 101404. [CrossRef]
10. Guo, L.; Wang, H.; Li, X.; Fei, G.; Yuan, Y.; Li, Y. A Synergistic System of Polyaniline@ Graphene-Alkyd Resin via a Gemini Surfactant for Enhanced Anti-Corrosion Properties. *Prog. Org. Coat.* **2022**, *170*, 106944. [CrossRef]
11. Deyab, M.A.; Eddahaoui, K.; Essehli, R.; Benmokhtar, S.; Rhadfi, T.; De Riccardis, A.; Mele, G. Influence of Newly Synthesized Titanium Phosphates on the Corrosion Protection Properties of Alkyd Coating. *J. Mol. Liq.* **2016**, *216*, 699–703. [CrossRef]
12. Benitha, V.S.; Jeyasubramanian, K.; Hikku, G.S. Investigation of Anti-Corrosion Ability of Nano Mixed Metal Oxide Pigment Dispersed Alkyd Coating and Its Optimization for A36 Steel. *J. Alloys Compd.* **2017**, *721*, 563–576. [CrossRef]

13. Alam, J.; Riaz, U.; Ahmad, S. High Performance Corrosion Resistant Polyaniline/Alkyd Ecofriendly Coatings. *Curr. Appl. Phys.* **2009**, *9*, 80–86. [CrossRef]
14. Ifijen, I.H.; Maliki, M.; Omorogbe, S.O.; Ibrahim, S.D. Incorporation of Metallic Nanoparticles Into Alkyd Resin: A Review of Their Coating Performance. In Proceedings of the TMS 2022 151st Annual Meeting & Exhibition Supplemental Proceedings, Anaheim, CA, USA, 27 February–3 March 2022; Springer International Publishing: Cham, Switzerland, 2022; pp. 338–349.
15. Jeyasubramanian, K.; Benitha, V.S.; Parkavi, V. Nano Iron Oxide Dispersed Alkyd Coating as an Efficient Anticorrosive Coating for Industrial Structures. *Prog. Org. Coat.* **2019**, *132*, 76–85. [CrossRef]
16. Wang, W.; Xu, L.; Li, X.; Lin, Z.; Yang, Y.; An, E. Self-Healing Mechanisms of Water Triggered Smart Coating in Seawater. *J. Mater. Chem. A* **2014**, *2*, 1914–1921. [CrossRef]
17. Neto, A.G.C.; Pellanda, A.C.; de Carvalho Jorge, A.R.; Floriano, J.B.; Berton, M.A.C. Preparation and Evaluation of Corrosion Resistance of a Self-Healing Alkyd Coating Based on Microcapsules Containing Tung Oil. *Prog. Org. Coat.* **2020**, *147*, 105874. [CrossRef]
18. Karekar, S.E.; Bagale, U.D.; Sonawane, S.H.; Bhanvase, B.A.; Pinjari, D.V. A Smart Coating Established with Encapsulation of Zinc Molybdate Centred Nanocontainer for Active Corrosion Protection of Mild Steel: Release Kinetics of Corrosion Inhibitor. *Compos. Interfaces* **2018**, *25*, 785–808. [CrossRef]
19. Li, W.; Hintze, P.; Calle, L.M.; Buhrow, J.; Curran, J.; Muehlberg, A.J.; Gelling, V.J.; Webster, D.C.; Croll, S.G.; Contu, F.; et al. *Smart Coating for Corrosion Indication and Prevention: Recent Progress*; OnePetro: Richardson, TX, USA, 2009.
20. Vijayan, P.P.; Al-Maadeed, M. Self-Repairing Composites for Corrosion Protection: A Review on Recent Strategies and Evaluation Methods. *Materials* **2019**, *12*, 2754.
21. Gupta, A.K.; Gupta, M. Synthesis and Surface Engineering of Iron Oxide Nanoparticles for Biomedical Applications. *Biomaterials* **2005**, *26*, 3995–4021. [CrossRef]
22. Yu, C.H.; Caiulo, N.; Lo, C.C.; Tam, K.; Tsang, S.C. Synthesis and Fabrication of a Thin Film Containing Silica-Encapsulated Face-Centered Tetragonal FePt Nanoparticles. *Adv. Mater.* **2006**, *18*, 2312–2314. [CrossRef]
23. Naser, A.A.; Al-Mubarak, A.S.; Al-Sawaad, H.Z. Synthesis, Characterization and Evaluation of Some Graphene Oxide Derivatives and Their Application as Corrosion Inhibitors for Carbon Steel Alloy Type C1025 in Hydrochloric Acid. *Int. J. Corros. Scale Inhib.* **2019**, *8*, 974.
24. Mohamed, M.G.; Mahdy, A.; Obaid, R.J.; Hegazy, M.A.; Kuo, S.-W.; Aly, K.I. Synthesis and Characterization of Polybenzoxazine/Clay Hybrid Nanocomposites for UV Light Shielding and Anti-Corrosion Coatings on Mild Steel. *J. Polym. Res.* **2021**, *28*, 297. [CrossRef]
25. Aly, K.I.; Abd El-Lateef, H.M.; Yehia, N.; Khodairy, A.; Sayed, M.M.; El-Remaily, M.A.E.A.A.A. Novel Polyesters Based on Indazole Moiety: Synthesis, Characterization and Applicability as Efficient Inhibitors for Acidic X-65-Steel Corrosion. *React. Funct. Polym.* **2021**, *166*, 105001. [CrossRef]
26. Aly, K.I.; Mahdy, A.; Hegazy, M.A.; Al-Muaikel, N.S.; Kuo, S.-W.; Gamal Mohamed, M. Corrosion Resistance of Mild Steel Coated with Phthalimide-Functionalized Polybenzoxazines. *Coatings* **2020**, *10*, 1114. [CrossRef]
27. Mohamed, M.G.; Kuo, S.W.; Mahdy, A.; Ghayd, I.M.; Aly Kamal, I. Bisbenzylidene Cyclopentanone and Cyclohexanone-Functionalized Polybenzoxazine Nanocomposites: Synthesis, Characterization, and Use for Corrosion Protection on Mild Steel. *Mater. Today Commun.* **2020**, *25*, 101418. [CrossRef]
28. Cayton, R.H.; Sawitowski, T. The Impact of Nano-Materials on Coating Technologies. In *Proceedings of the Technical Proceedings of the 2005 NSTI Nanotechnology Conference and Trade Show*; NSTI: Mumbai, India, 2005; Volume 2, pp. 8–12.
29. Fernando, R. Nanomaterial Technology Applications in Coatings. *JCT Coat.* **2004**, *1*, 32–38.
30. Riaz, U.; Ahmad, S.; Ashraf, S.M. Comparison of Corrosion Protective Performance of Nanostructured Polyaniline and Poly(1-Naphthylamine)-Based Alkyd Coatings on Mild Steel. *Mater. Corros.* **2009**, *60*, 280–286. [CrossRef]
31. Jadhav, R.S.; Hundiwale, D.G.; Mahulikar, P.P. Synthesis of Nano Polyaniline and Poly-o-Anisidine and Applications in Alkyd Paint Formulation to Enhance the Corrosion Resistivity of Mild Steel. *J. Coat. Technol. Res.* **2010**, *7*, 449–454. [CrossRef]
32. Sweeton, F.H.; Baes, C.F., Jr. The Solubility of Magnetite and Hydrolysis of Ferrous Ion in Aqueous Solutions at Elevated Temperatures. *J. Chem. Thermodyn.* **1970**, *2*, 479–500. [CrossRef]
33. Mahmoud Zaghloul, M.Y.; Yousry Zaghloul, M.M.; Yousry Zaghloul, M.M. Physical Analysis and Statistical Investigation of Tensile and Fatigue Behaviors of Glass Fiber-Reinforced Polyester via Novel Fibers Arrangement. *J. Compos. Mater.* **2023**, *57*, 147–166. [CrossRef]
34. Zaghloul, M.M.Y.M. Mechanical Properties of Linear Low-Density Polyethylene Fire-Retarded with Melamine Polyphosphate. *J. Appl. Polym. Sci.* **2018**, *135*, 46770. [CrossRef]
35. Mahmoud Zaghloul, M.Y.; Yousry Zaghloul, M.M.; Yousry Zaghloul, M.M. Developments in Polyester Composite Materials–An in-Depth Review on Natural Fibres and Nano Fillers. *Compos. Struct.* **2021**, *278*, 114698. [CrossRef]
36. Zaghloul, M.M.Y.; Zaghloul, M.Y.M.; Zaghloul, M.M.Y. Experimental and Modeling Analysis of Mechanical-Electrical Behaviors of Polypropylene Composites Filled with Graphite and MWCNT Fillers. *Polym. Test.* **2017**, *63*, 467–474. [CrossRef]
37. Zaghloul, M.M.Y.; Steel, K.; Veidt, M.; Heitzmann, M.T. Wear Behaviour of Polymeric Materials Reinforced with Man-Made Fibres: A Comprehensive Review about Fibre Volume Fraction Influence on Wear Performance. *J. Reinf. Plast. Compos.* **2022**, *41*, 215–241. [CrossRef]

38. Zaghloul, M.M.Y.; Steel, K.; Veidt, M.; Heitzmann, M.T. Mechanical and Tribological Performances of Thermoplastic Polymers Reinforced with Glass Fibres at Variable Fibre Volume Fractions. *Polymers* **2023**, *15*, 694. [CrossRef]
39. Fuseini, M.; Zaghloul, M.M.Y. Investigation of Electrophoretic Deposition of PANI Nano Fibers as a Manufacturing Technology for Corrosion Protection. *Prog. Org. Coat.* **2022**, *171*, 107015. [CrossRef]
40. Kulandaivalu, S.; Zainal, Z.; Sulaiman, Y. A New Approach for Electrodeposition of Poly (3, 4-Ethylenedioxythiophene)/Polyaniline (PEDOT/PANI) Copolymer. *Int. J. Electrochem. Sci.* **2015**, *10*, 8926–8940. [CrossRef]
41. Jeyakumari, J.J.L.; Yelilarasi, A.; Sundaresan, B.; Dhanalakshmi, V.; Anbarasan, R. Chemical Synthesis of Poly (Aniline-Co-o/m-Toluidine)/V_2O_5 Nano Composites and Their Characterizations. *Synth. Met.* **2010**, *160*, 2605–2612. [CrossRef]
42. Zhang, Y.; Shao, Y.; Meng, G.; Zhang, T.; Li, P.; Wang, F. Evaluation of the Corrosion Protection of Defective Polyaniline/Epoxy Coating by Localized Electrochemical Impedance Spectroscopy. *J. Coat. Technol. Res.* **2015**, *12*, 777–785. [CrossRef]
43. Mahudeswaran, A.; Manoharan, D.; Chandrasekaran, J.; Vivekanandan, J.; Vijayanand, P.S. CSA Doped Poly (Aniline-Co-o-Toluidine) and Dispersed Zinc Oxide Nanoparticles: A Promising Material for Photovoltaics. *Mater. Res.* **2015**, *18*, 482–488. [CrossRef]
44. Shirinova, H.A.; Palma, L.D.; Sarasini, F. Synthesis and Characterization of Magnetic Nanocomposites for Environmental Remediation. *Chem. Eng.* **2016**, *47*. [CrossRef]
45. Petcharoen, K.; Sirivat, A. Magneto-Electro-Responsive Material Based on Magnetite Nanoparticles/Polyurethane Composites. *Mater. Sci. Eng. C* **2016**, *61*, 312–323. [CrossRef] [PubMed]
46. Bian, L.; Bao, L.; Wang, J.; Lei, J. In Situ Preparation of Monodispersed Ag/Polyaniline/Fe_3O_4 Nanoparticles via Heterogeneous Nucleation. *Nanoscale Res. Lett.* **2013**, *8*, 309. [CrossRef] [PubMed]
47. Zarrouk, A.; Bentiss, F. Evaluation of Alkaloids Extract of *Retama monosperma* (L.) Boiss. Stems as a Green Corrosion Inhibitor for Carbon Steel in Pickling Acidic Medium by Means of Gravimetric, AC Impedance and Surface Studies. *J. Mater. Environ. Sci.* **2017**, *9*, 358–369.
48. Simonović, A.T.; Tasić, Ž.Z.; Radovanović, M.B.; Petrović Mihajlović, M.B.; Antonijević, M.M. Influence of 5-Chlorobenzotriazole on Inhibition of Copper Corrosion in Acid Rain Solution. *ACS Omega* **2020**, *5*, 12832–12841. [CrossRef]
49. Ansari, K.R.; Quraishi, M.A.; Singh, A. Pyridine Derivatives as Corrosion Inhibitors for N80 Steel in 15% HCl: Electrochemical, Surface and Quantum Chemical Studies. *Measurement* **2015**, *76*, 136–147. [CrossRef]
50. Lgaz, H.; Lee, H. Facile Preparation of New Hydrazone Compounds and Their Application for Long-Term Corrosion Inhibition of N80 Steel in 15% HCl: An Experimental Study Combined with DFTB Calculations. *J. Mol. Liq.* **2022**, *347*, 117952. [CrossRef]
51. Zaher, A.; Aslam, R.; Lee, H.-S.; Khafouri, A.; Boufellous, M.; Alrashdi, A.A.; El Aoufir, Y.; Lgaz, H.; Ouhssine, M. A Combined Computational & Electrochemical Exploration of the *Ammi visnaga* L. Extract as a Green Corrosion Inhibitor for Carbon Steel in HCl Solution. *Arab. J. Chem.* **2022**, *15*, 103573. [CrossRef]
52. Dehghani, A.; Bahlakeh, G.; Ramezanzadeh, B.; Ramezanzadeh, M. Electronic/Atomic Level Fundamental Theoretical Evaluations Combined with Electrochemical/Surface Examinations of Tamarindus Indiaca Aqueous Extract as a New Green Inhibitor for Mild Steel in Acidic Solution (HCl 1 M). *J. Taiwan Inst. Chem. Eng.* **2019**, *102*, 349–377. [CrossRef]
53. Saha, S.K.; Murmu, M.; Murmu, N.C.; Banerjee, P. Benzothiazolylhydrazine Azomethine Derivatives for Efficient Corrosion Inhibition of Mild Steel in Acidic Environment: Integrated Experimental and Density Functional Theory Cum Molecular Dynamics Simulation Approach. *J. Mol. Liq.* **2022**, *364*, 120033. [CrossRef]
54. Saha, S.K.; Dutta, A.; Ghosh, P.; Sukul, D.; Banerjee, P. Adsorption and Corrosion Inhibition Effect of Schiff Base Molecules on the Mild Steel Surface in 1 M HCl Medium: A Combined Experimental and Theoretical Approach. *Phys. Chem. Chem. Phys.* **2015**, *17*, 5679–5690. [CrossRef]
55. Umoren, S.A.; Solomon, M.M.; Obot, I.B.; Suleiman, R.K. Date Palm Leaves Extract as a Green and Sustainable Corrosion Inhibitor for Low Carbon Steel in 15 Wt.% HCl Solution: The Role of Extraction Solvent on Inhibition Effect. *Environ. Sci. Pollut. Res.* **2021**, *28*, 40879–40894. [CrossRef]
56. Solomon, M.M.; Umoren, S.A.; Quraishi, M.A.; Jafar Mazumder, M.A. Corrosion Inhibition of N80 Steel in Simulated Acidizing Environment by N-(2-(2-Pentadecyl-4,5-Dihydro-1H-Imidazol-1-YL) Ethyl) Palmitamide. *J. Mol. Liq.* **2019**, *273*, 476–487. [CrossRef]
57. Naderi, R.; Attar, M.M. Electrochemical Study of Protective Behavior of Organic Coating Pigmented with Zinc Aluminum Polyphosphate as a Modified Zinc Phosphate at Different Pigment Volume Concentrations. *Prog. Org. Coat.* **2009**, *66*, 314–320. [CrossRef]
58. Abdel-Gaber, A.M.; Abd-El Nabey, B.A.; Khamis, E.; Abdelattef, O.A.; Aglan, H.; Ludwick, A. Influence of Natural Inhibitor, Pigment and Extender on Corrosion of Polymer Coated Steel. *Prog. Org. Coat.* **2010**, *69*, 402–409. [CrossRef]
59. Yeh, J.-M.; Hsieh, C.-F.; Yeh, C.-W.; Wu, M.-J.; Yang, H.-C. Organic Base-Catalyzed Sol–Gel Route to Prepare PMMA–Silica Hybrid Materials. *Polym. Int.* **2007**, *56*, 343–349. [CrossRef]
60. Zhang, X.; Wang, F.; Du, Y. Effect of Nano-Sized Titanium Powder Addition on Corrosion Performance of Epoxy Coatings. *Surf. Coat. Technol.* **2007**, *201*, 7241–7245. [CrossRef]
61. Pavithra, M.K.; Venkatesha, T.V.; Kumar, M.K.P.; Anantha, N.S.R. Outstanding Inhibitive Effect of Colchicine on Aluminium Alloy 6061 Corrosion. *J. Electrochem. Sci. Eng.* **2015**, *5*, 197–208. [CrossRef]
62. Zhu, C.; Xie, R.; Xue, J.; Song, L. Studies of the Impedance Models and Water Transport Behaviors of Cathodically Polarized Coating. *Electrochim. Acta* **2011**, *56*, 5828–5835. [CrossRef]

63. Petcharoen, K.; Sirivat, A. Synthesis and Characterization of Magnetite Nanoparticles via the Chemical Co-Precipitation Method. *Mater. Sci. Eng. B* **2012**, *177*, 421–427. [CrossRef]
64. Baig, N.; Chauhan, D.S.; Saleh, T.A.; Quraishi, M.A. Diethylenetriamine Functionalized Graphene Oxide as a Novel Corrosion Inhibitor for Mild Steel in Hydrochloric Acid Solutions. *New J. Chem.* **2019**, *43*, 2328–2337. [CrossRef]
65. Gupta, R.K.; Malviya, M.; Verma, C.; Quraishi, M.A. Aminoazobenzene and Diaminoazobenzene Functionalized Graphene Oxides as Novel Class of Corrosion Inhibitors for Mild Steel: Experimental and DFT Studies. *Mater. Chem. Phys.* **2017**, *198*, 360–373. [CrossRef]